Optimization of welding parameters for improving welded joints used in rolling stock structures using experimental and Taguchi technique

Sampath Suranjan Salins[1] · **Deepak Inder Kumar**[1] · **H. K. Sachidananda**[1]

Abstract

Manufacturing involves cutting, machining, and joining processes for making all the mechanical structures in the world. Welding is a joining process where a lot of input variables are involved to achieve good mechanical properties and able to withstand load and stresses during its service. This study presents the effect of welding current, welding speed, and shielding gas flow rate on hardness and ultimate tensile strength in gas metal arc welding which is commonly used in car body structures in railway industries. The response of these process parameters has been analyzed and optimized using the Taguchi method. This study helps to understand root cause analysis of welding defects or to control the process parameters to improve welding joints used in rolling stock structures. From the experimental study it is observed that the optimum process parameters for ultimate tensile strength are 300 amp for welding current, 3 mm/min for welding speed and 10 L/min for gas flow rate for tensile strength and optimum value for hardness is 200 amp for welding current, 4 mm/min for welding speed and 20 L/min for gas flow rate.

Keywords Rolling stock · Gas metal arc welding · Hardness number · Tensile strength · Taguchi method

Abbreviations

BHN	Brinell hardness number (MPa)
DOE	Design of experiments
HAZ	Heat effected zone
MIG	Metal inert gas
CFD	Computational fluid dynamics
TIG	Tungsten inert gas
UTM	Universal testing machine
FIE	Fuel instruments and engineers
ANSI	American Iron and Steel Institute

I	Current (amps)
R	Resistance (Ω)
L	Length of the plate (m)
B	Breadth of the plate (m)
X	Independent variables
y	Uncertainty intervals
W_R	Dependent variable
U	Function
S/N	Stress versus number of cycles
y_j	Value of the characteristic
j	Observation
R	Number of observations

List of symbols

P	Load (Kgf)
D	Steel ball diameters (mm)
d	Depression diameter (mm)
V	Voltage (V)

✉ H. K. Sachidananda
sachidananda@manipaldubai.com

1 School of Engineering and IT, Manipal Academy of Higher Education, Dubai, UAE

1 Introduction

Welding is one of the most common processes of fabricating large structures used in any industry as it is cost effective and the most flexible method of joining. So, the demand for reliability and improved integrity is the major challenges faced in industries as Suggested by Charles et al. [1]. The quality of the weld obtained depends on welding parameters such as welding current, welding speed, voltage, feed rate, speed

of welding, gas flow rate etc., apart from welding output parameters such as weld depth, depth of penetration, tensile strength, hardness, impact strength etc. as presented by Tsung and Yen [2]. The shielding gas in case of welding plays an important role during the welding process and the gas compositional modification has direct impact on welding parameters as suggested by Masahiro et al. [3]. The welding parameters have direct impact on structure and properties of the material as reviewed by Harsh et al. [4]. As the welding current increases the amount of melting increases in the base metal which helps to increase the weld nugget width which in turn increases the bonding strength and correspondingly tensile shear force increases as mentioned by Yemelyushin et al. [5]. At the same time, the welding speed reduces the nugget width, and the root weld is reduced due to rise in welding speed and low heat input as presented by Mei et al. [6]. The effect of shielding gas is to safeguard the welding from exposure to oxygen, nitrogen, and hydrogen to prevent porosity and excessive spatter as mentioned by Wichan and Loeshphan [7]. The shielding gas during the MIG welding process considering different shielding gases and its effect on hardness and tensile strength have shown improvement in mechanical properties and corrosion resistance of the material by adding 2% of oxygen in Argon shielding gas as mentioned by Xin et al. [8]. Various researchers have studied the influence of different operational parameters on the welded joint.

Ajit et al. [9] evaluated surface modelling considering AISI 1040 medium carbon steel to investigate the tensile strength of metal inert gas (MIG) welding. They considered the different process parameters such as current, wire feed rate, voltage, and gas flow rate. They concluded by optimizing the tensile strength for the various process parameters. The empirical relations they developed can be used to estimate yield strength in the case of AISI 1040 medium carbon steel. Chinakhov et al. [10] analyzed the influence of shielding gas flow rate on electron metal drops. They studied metal drops of molten electrode metal and their influence on basic forces and force of gas dynamics impact. They concluded that changes were observed in chemical composition based on transfer frequency of electrode metal drop. They showed that gas flow rate has a significant impact on electrode metal drop and the chemical composition of the weld metal. Xiaoyi et al. [11] evaluated the shielding gas effect on welding parameters in the case of laser-arc hybrid welding and MIG welding. They studied the influence of shielding gas using computational fluid dynamics analysis (CFD) with high-speed photography. They concluded that the process stability of MIG welding is poor as compared to laser-arc hybrid welding. These results show that shielding gas composition and shielding gas flow have significant impact during welding. Liu et al. [12] studied microstructure and corrosion resistance by considering laser-arc hybrid

welding. The weld surface of high nitrogen steel was analyzed by changing the flow rate of nitrogen. They concluded that corrosion resistance is not affected by nitrogen flow. Maros et al. [13] determined the process parameters effect on the microstructure and mechanical properties considering aluminum welded laser joints. The effect of process parameters considering ambient atmosphere gas flow rate by a mixture of argon and helium were determined. Optimizing of the parameters shows that no cracks and pores were found in the shielded weld metal and from the results they showed that the gas flow rate plays an important role during welding process. Rahman et al. [14] found the impact of argon gas flow rate and its effect on hardness of welded joint. The effect of gas flow rate on thickness of 3 mm thickness mild steel plate considering different flow rates were studied. This research work concluded that high gas flow rate induces sudden solidification of weld joint, and it reduces the possibility of escape of air from the weld pool. Ashish et al. [15] depicted the mechanical and microstructure properties using TIG welding. Optimization of TIG welding considering the design of experiments and Grey Taguchi method were carried out. It considered various input parameters such as welding current, welding gas and welding voltage. This work concluded that using optimum welding parameters yielded best results in terms of hardness and tensile strength. Leander et al. [16] analyzed the spatter formation in case of deep penetration welding during increased welding speeds using gas flow rate. Effect of gas flow rate considering argon gas on welding stainless steel was evaluated. This work concluded that further investigation is needed to study the effect of gas flow rate on spatter formation. Anteneh et al. [17] studied the welding process parameters such as welding current, gas flow rate, root gap and filler materials and its effect on TIG welding. Microstructure was analyzed and the tensile strength, hardness, and flexural strength were determined for stainless steel and carbon steel material. Research work concluded that optimized results improved the performance by 22.90%. They showed that welding current is the crucial factor, and its impact is more on hardness of the specimen. Rizvi and Tewari [18] analyzed the influence of the voltage, current, speed and shielding gas flow rate. They analyzed the mechanical properties considering structural steel material and observed the microstructure changes. This work focused on the tensile fracture by seeing these structural steel samples in scanning electron microscope. This helped us to understand the effect of different variables with brittle materials. This work infers that microhardness values changed with gas flow rate.

From the above literatures it is seen that researchers have studied tensile strength, ultimate strength, hardness, and flexural strength etc. for various engineering materials in welding considering different welding parameters, but the research related to car body structures and its effects on various parameters are very limited especially in case of railway body

structural application. The study of welding in the case of car body structures is important as 40% of welding process is involved during the manufacturing process of railway structures. This study is important from the aspect of reducing the railway breakdown due to defects in the welding process [19, 20]. Also, the optimization of these parameters in the case of car body structures (railways) are limited and in this research Taguchi optimization has been used to evaluate the importance of different parameters during welding of mild steel part.

To overcome these gaps, a study of the welding parameters (Current, speed and gas flow rate) has been considered in case of rolling stock structures in railways. The cause of these welding parameters needs to be investigated and optimization process considering different welding parameters needs to be analyzed using Taguchi method.

The organization of the article starts with the framework of the car body structure used in railway industries and the dimensional details of the part manufactured for experimentation, welding parameters considered for the study. The next section discusses the tensile strength and hardness when the welding current is varied. Similarly, the next section discusses the tensile strength and hardness and how the welding current and gas flow rate affects these parameters. In the next section the Taguchi design of experiments considered for the study to optimize the various welding parameters and was followed by conclusions.

2 Methodology

Rolling stock car body shell as shown in Fig. 1 consists of two bent side structures, ends, roofs and underframe as presented by Takeshi et al. [21]. Each part is welded together to form one car body shell. The framework of a typical car body structure is shown in the Fig. 2. Which gives detailed information of the various thickness of the child part of a typical rolling car body structure. These car body structures are made by welding various sheet metal components with its thickness of ranging from 0.8 to 3 mm thickness. In this present work, sheet metal made of mild steel of 1 mm thickness which is the highest thickness of sheet metal used in above rolling stock structure. Eighteen test specimens are being produced using die punching process for the experimentation and the dimensional details of the mild steel part used for the study is as shown in Fig. 3. The chemical composition of the mild steel used for the study is as shown in Table 1.

Figure 4 shows the samples produced in workshop. These sheet metal plates are welded to produce 9 welded joints and a single unit. These welded joints are studied by altering the operational parameters such as gas flow rate, current and the speed. (Refer Table 2). Figure 5 shows the welded test specimen for experimentation and the dimensional detail of the

specimen welded for experimentation is as shown in Fig. 6. After the manufacturing of the 9 test specimens, the hardness and tensile tests were performed on the specimen to analyse the effect of welding parameters.

3 Experimental test rig specifications

Hardness measurement has been performed on welded joint for each sample by using Brinell hardness tester. The major specifications of the Brinell hardness tester are, test loads ranges from 10 to 3000 Kgf, it has Load accuracy of 0.05%, elevating screw stroke is 150 mm and measuring head with indenter vertical stroke is 30 mm. Tensile tests of the welding specimen is conducted on the universal testing machine (UTES-10 FIE make) which has a load capacity of 100 kN, load resolution 5 N, ram stroke of 150 mm, piston speed of 0–300 mm/min, power of 1.33 HP, Voltage of 400–440 V and maximum clearance between supports is 500 mm. Figure 7 shows the Brinell hardness testing machine and universal testing machine used for measuring Brinell hardness and ultimate tensile strength of the specimen. The results of all the above-mentioned tests have been analysed and explained in following section.

4 Instrumentation and uncertainty analysis

The measuring instruments used in the present research work and their specifications are described in Table 3.

The information processing (input and output) parameters are calculated based on several measurements; a certain error is expected which in turn influences the output parameters. The uncertainty analysis determines the result reliability of an engineering problem, without which, the performance cannot be evaluated.

Let X_1, X_2…Xn be the independent variables distributed normally and y_1, y_2…y_n be the uncertainty intervals. U be the function. The Uncertainty of dependent variable w_R is calculated as given by Eq. (1)

$$w_R = \left[\left(\frac{\delta U}{\delta X_1}y_1\right)^2 + \left(\frac{\delta U}{\delta X_2}y_2\right)^2 + \left(\frac{\delta U}{\delta X_3}y_3\right)^2 \right.$$
$$\left. + \cdots + \left(\frac{\delta U}{\delta X}w_n\right)^2\right]^{0.5} \tag{1}$$

The uncertainty values obtained for the dependent variables is shown in Table 4.

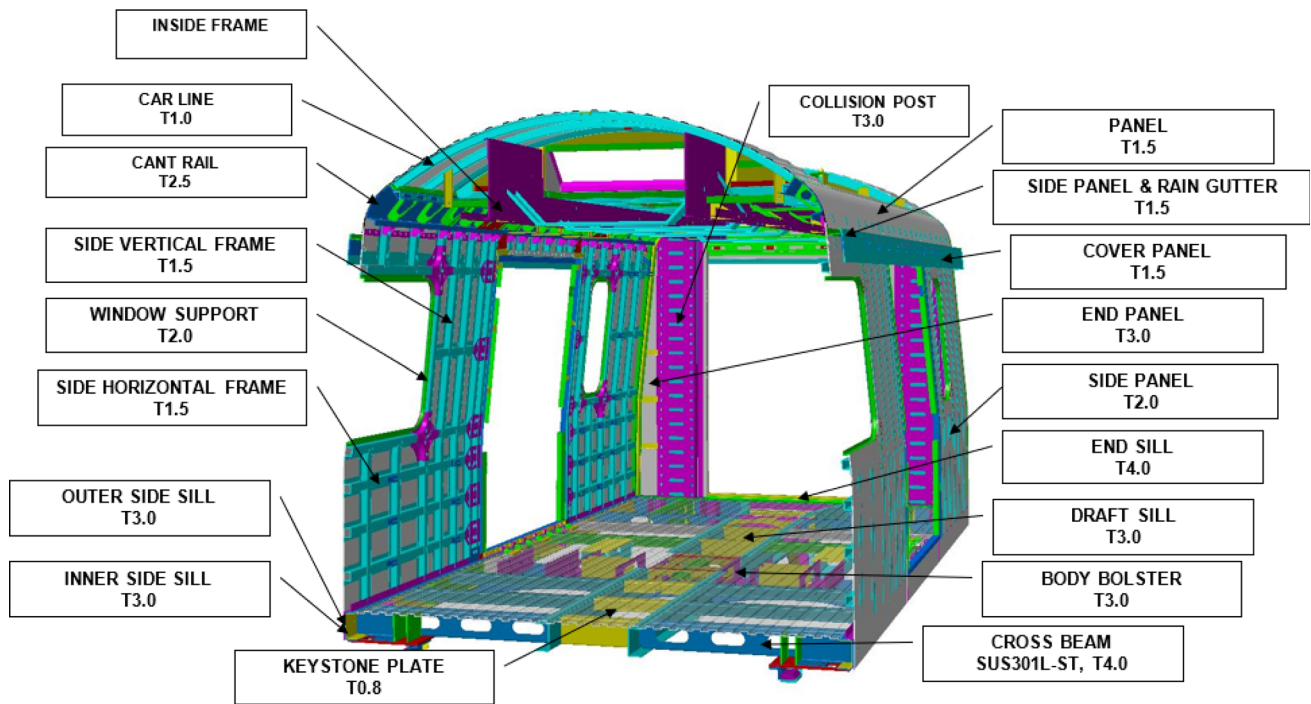**Fig. 1** Metro train of steel car body structure

Fig. 2 Framework of car body structure

Current is defined as a ratio of the voltage to the resistance. Resistance is given by the unit Ω.
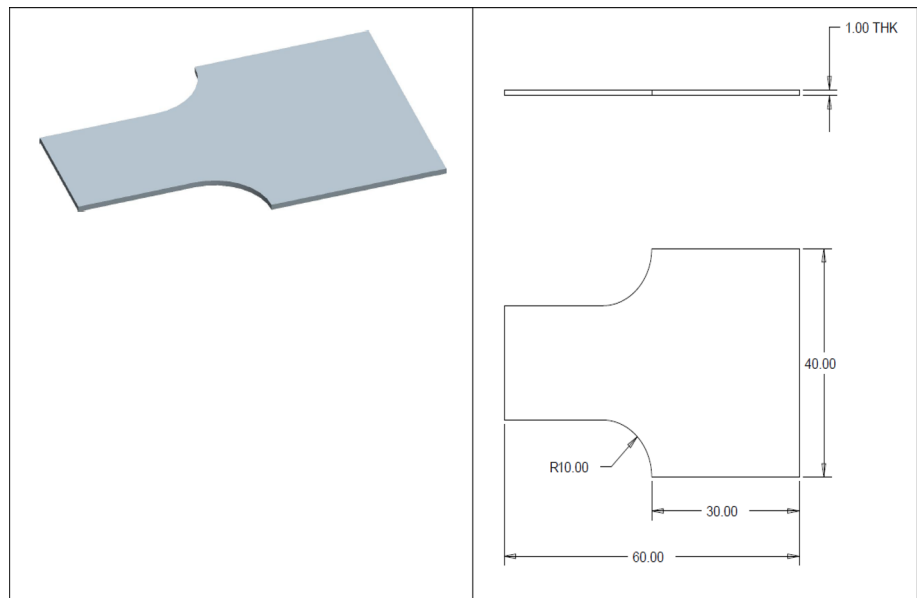
$$I = \frac{V}{R}$$

Uncertainty in the current measurement

$$\frac{\partial(I)}{I} = \sqrt{\left(\frac{\partial V}{V}\right)^2 + \left(-\frac{\partial R}{R}\right)^2} \tag{2}$$

Tensile strength is the ratio of the maximum force applied to the original area of cross section. P is the force (maximum)

Fig. 3 Dimensional details of mild sheet metal part


Table 1 Chemical Composition of Mild Steel

Iron (%)	Manganese (%)	Sulphur (%)	Phosphorus (%)	Carbon (%)
98.82–99.34	0.6–0.8	0.05	0.04	0.14–0.2

Fig. 4 Samples produced in workshop

Table 2 Welding parameters considered for various samples

Sample No	Welding on plates	Gas flow rate (L/min)	Current (amp)	Speed (mm/min)
1	1–2	20	100	4
2	3–4	10	100	3
3	5–6	15	100	5
4	7–8	20	200	4
5	9–10	10	200	3
6	11–12	15	200	5
7	13–14	20	300	4
8	15–16	10	300	3
9	17–18	15	300	5
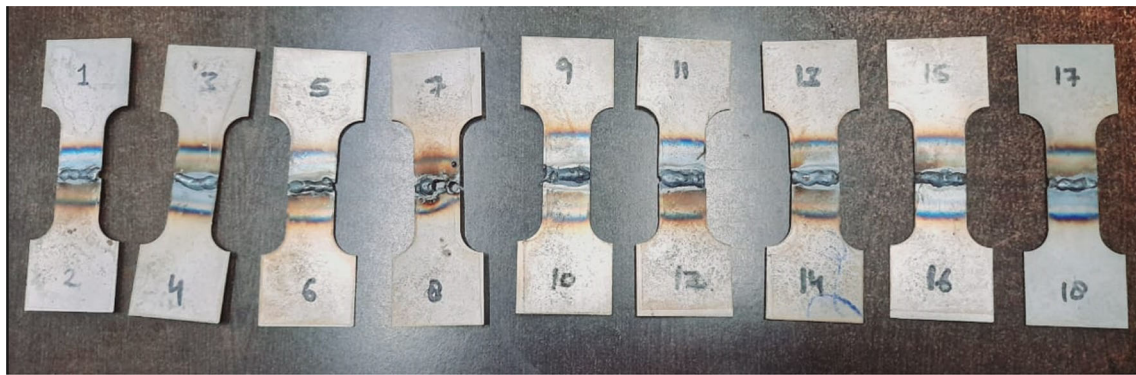
Fig. 5 Welded test specimen
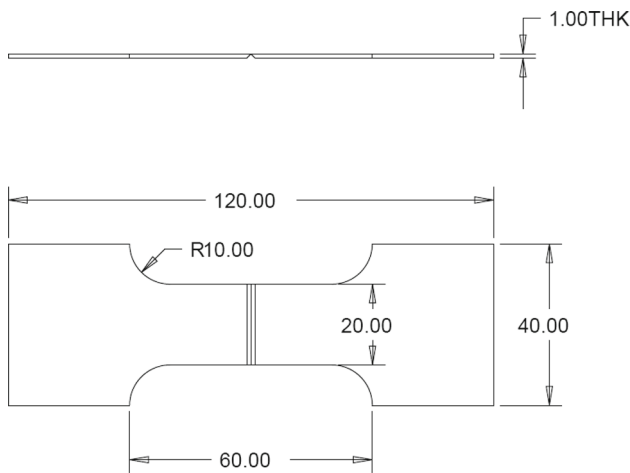
Fig. 6 Dimensional details of welded steel specimen

applied in N, L and B is the length and breadth of the plate in m.

$$\sigma = \frac{P}{L \times B} \tag{3}$$

Uncertainty in the tensile strength is

$$\frac{\partial(\sigma)}{\sigma} = \sqrt{\left(\frac{\partial P}{P}\right)^2 + \left(-\frac{\partial L}{L}\right)^2 + \left(-\frac{\partial B}{B}\right)^2} \tag{4}$$

The Brinell hardness number is defined as a measure of the material hardness by pressing steel indenter on the work surface. It is expressed by the ratio of the maximum load to the area of depression made by the indenter. D is the diameter of the steel ball indenter in m and d is the diameter of the depression in m.

$$BHN = \frac{2P}{\pi D(D - (D^2 - d^2)} \tag{5}$$

Uncertainty in the tensile strength is

$$\frac{\partial(BHN)}{BHN} = \sqrt{\left(\frac{\partial P}{P}\right)^2 + \left(-\frac{\partial D}{D}\right)^2 + \left(-\frac{\partial D}{D}\right)^2} \tag{6}$$

Uncertainties values which are calculated are below 5%, hence the error relating to the measurement of the output parameters are minimum. Input and output parameters are used to evaluate the performance parameters which is discussed in next section.

Fig. 7 Blue star Brinell hardness tester and FIE make universal testing machine UTES-10
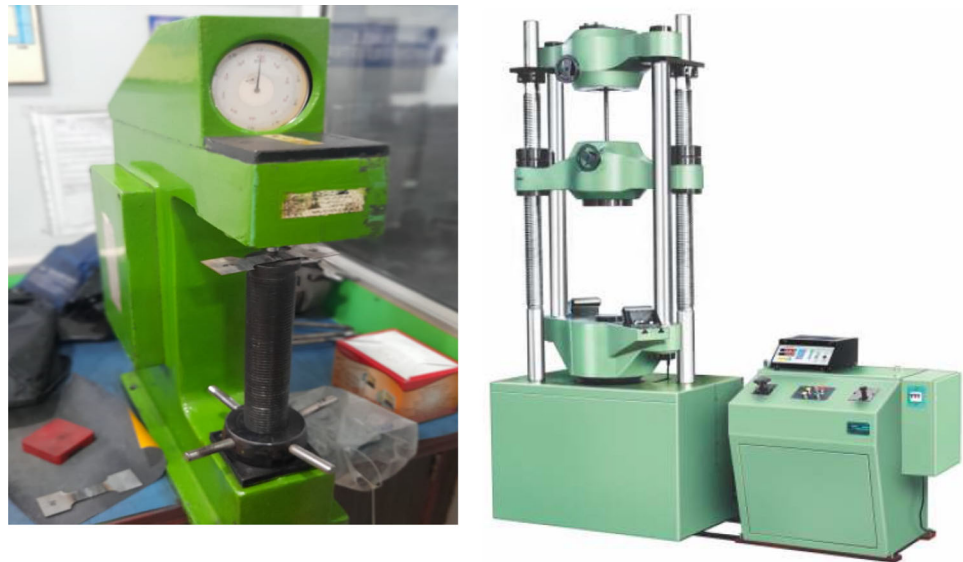
Table 3 Measuring sensors

| To Measure	Name of the instrument	Specifications
Yield stress	Universal testing machine	UTES-10 FIE make, load resolution 5 N, maximum load of 100 kN, ram stroke 150 mm piston speed 0–300 mm/min, power 1.33 HP
Hardness	Brinell hardness tester	Load range 10–3000 Kgf, load accuracy 0.05%, Screw stroke 150 mm
Voltage and Current	Clamp Meter	Power supply (2 × 1.5 V) AAA battery Operating temperature (0–40 °C, < 75%RH) Storage temperature (10–50 °C, < 80%RH) Manufacturer: UNI-T

Table 4 Uncertainty values for dependent variables

S.No	Variable	Percentage uncertainty (%)
1	Yield stress	1.75
2	Hardness number	1.70
3	Current	1.05

5 Results and discussions

5.1 Hardness

Figure 8 (Refer graph A) shows changes in hardness of test specimen due to change in welding current at shielding gas
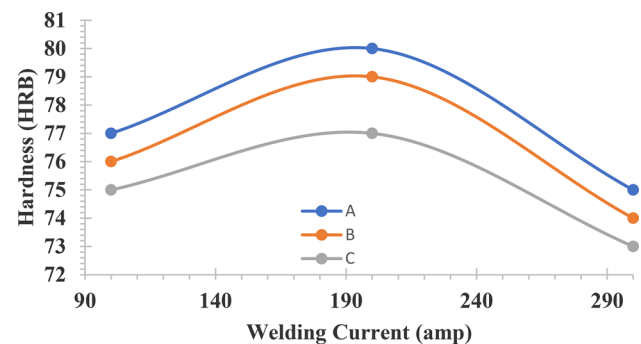
Fig. 8 Change of hardness with varying current. **A**—Gas flow rate 20 L/min, welding speed 4 mm/min, **B**—Gas flow rate 10 L/min, welding speed 3 mm/min **C**—Gas flow rate 15 L/min, welding speed 5 mm/min

flow rate of 20 L/min and welding speed of 4 mm/min. The hardness of the microstructure of the welds alters with respect to the gas flow rate and welding speed. The various microstructural changes defects like formation of martensite, coarsening of grain and precipitation of carbide changes the hardness of the material as gas flow rate and welding speed increases. This in turn changes the fracture toughness of the material and has a high chance of brittle fracture as mentioned by Rizvi and Tewari [18]. From the literatures it is also seen that changes in the welding speed rises the hardness of the weld. This occurs, as the welding speed increases, less heat will be generated in the weld area and results in the rise of hardness of the material (Bekir and Behcet [22]). From Fig. 8 (Graph A) it is also observed that the maximum hardness is achieved (due to intense heat and proper fusing of the material).

Figure 8 (Graph B) shows change of Brinell hardness of test specimens with changes in welding current for a gas

flow rate of 10 L/min, and for welding speed of 3 mm/min. It is noticed that as the gas flow rate rises, the molten metal pool will protect the material and it is possible to achieve smooth welding. Similarly, if the gas flow rate decreases there is a possibility of atmospheric contamination which in turn results in porosity and oxidation. Also, gas flow rate depends on whether the flow is turbulent during welding and if it so results in porosity of the weld. The hardness in this combination is lower than earlier scenario, and occurs due to lower welding speed, the penetration of the welding arc is satisfactory, and hence the weld pool is sturdy and ductile leading to lower hardness. At 200 amp, it is observed that the hardness is slightly higher than that of the previous case despite reduction in gas flow rate (20–10 L/min). This has happened due to reduction in the welding speed (4–3 mm/s). This indicates that speed of welding and gas flow rate have greater impact on the welding and its defects.

Figure 8 (Graph C) shows change in hardness of test specimens for change in welding current (gas flow rate of 15 L/min and welding speed 5 mm/min). In this case the average hardness value is less than other cases considered which occurs due to increased welding speed which in turn leads to poor penetration, reduce in load carrying capacity as the weld metal fails to fuse, and presence of cavities caused due to freezing of gas as presented by Muyu et al. [23].

From the above discussion it is observed that the welding speed impact the quality of the weld. This demonstrates that welding speed need to be appropriate during welding various materials used in industries otherwise, the possibility of imperfection such as burn through of base metal, and improper penetration cannot be ruled out.

5.2 Shielding gas flow rate effect on hardness

The major effect of shielding gas is to prevent the entry of atmospheric oxygen and nitrogen into the weld pool. The exposure and reaction with these gases leads to welding defects such as porosity (holes with the weld bead), inclusions in terms of non-metallic particles trapped in the welding material and cracking of weld. The arc characteristics, the transfer of filler material, depth of fusion between base metal, welding speed and in turn mechanical properties are influenced by gas and gas flow rate.

Figure 9 (Graph A) shows change in hardness of test specimens with gas flow rate at 200 amp. From the theory of welding process, it is understood that as the current increases during welding results in greater melting of base metal and in turn will widen the weld bead resulting in more bonding strength of atoms which also increases the tensile shear force as mentioned by Panji et al. [24]. Figure 9 (Graph B) shows change of hardness of test specimens with gas flow rate at 100 amp. The highest hardness is achieved for a gas flow rate of 21 L/min. So, increase in gas flow rate helps to protect the
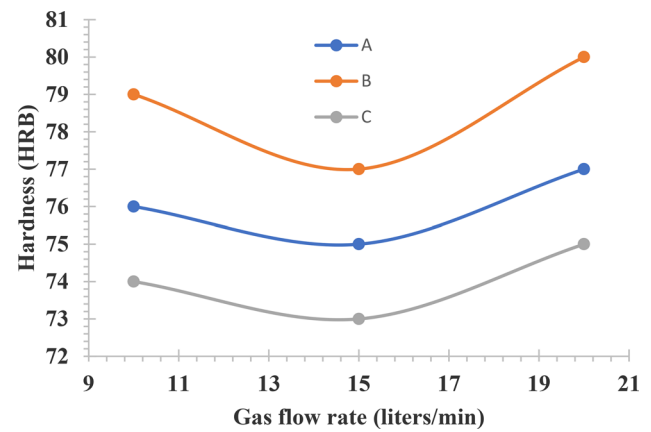

Fig. 9 Hardness variation with gas flow rate. **A**—Gas flow rate at 200 amp, **B**—Gas flow rate at 100 amp, **C**—Gas flow rate at 300 amp

weld and weld material against atmospheric contamination and in turn helps to achieve higher quality weld. The average hardness in above case is more as compared to the earlier cases considered.

Figure 9 (Graph C) reveals the changes of hardness for specimens with respect to changes in gas flow rate at 300 amp. In this case it is observed that the hardness is reducing from 10 to 15 L/min of gas flow rate and the hardness of the weld specimen increases from 15 to 20 L/min gas flow rate.

From Fig. 9 (for all cases) it is observed that the hardness decreases from gas flow rate of 10–15 L/min and then it increases from 15 to 20 L/min. From this it is understood that there is an optimum value of current from which it is possible to achieve higher hardness or lower hardness for a specific value of gas flow rate. Also, as the welding current increases from 100 amp to 300-amp results in increased hardness in all the cases of graphs after the gas flow rate of 15 L/min (changed from 75 to 77 BHN in case of Fig. 9 Graph A, increased from 77 to 80 BHN in case of Fig. 9 Graph B and 73 BHN to 75 BHN in case of Fig. 9 Graph C). Also, flow rate should be kept sufficiently high to achieve good quality weld. In this case of Fig. 9 it is observed that the changes in gas flow rate of 14–16 L/min is optimum otherwise, it will create more turbulence if the flow rate increases and in turn creates welding defects.

5.3 Welding speed effect on hardness

If the travel speed of the weld is raised the penetration of the weld inside the base material also increases [25]. At decreased travel speed the arc produced during welding is right above the centre of the weld metal pool and possibility of welding defect such as molten metal not completely reacting with cold surface of the base metal will in turn lead to cold lap. Also, the transfer of filler material to the weld pool will deposit on top of the metal, which is already deposited, and it
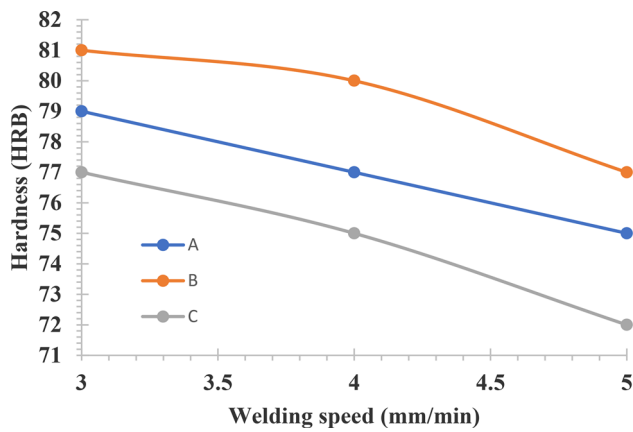
Fig. 10 Hardness variation with welding speed **A**—200 amp, **B**—100 amp, **C**—300 amp

Fig. 11 Changes of tensile strength with welding current **A**—welding current at, 10 L/min flow rate, 3 mm/min speed, **B**—welding current at, 20 L/min flow rate, 4 mm/min speed, **C**—welding current at, 15 L/min flow rate, 5 mm/min speed

reduces the metal droplet to penetrate the base material. Similarly, if the travel speed of the weld material is faster results in arc passing through the foremost edge of the weld pool and directly impacting the base material leaving the weld pool. This effects in deeper penetration of weld in the base metal which reduces the damping effect of the weld pool as described by Ahmad et al. [26].

Figure 10 (Graph A) shows the changes of hardness with welding speed at 200 amp. From this Graph A it is observed that hardness decreases with increase in welding speed. This occurs due to difference in cooling rate created at different weld speeds as mentioned by Morakabiyan et al. [27]. Figure 10 (Graph B) shows the variation in hardness with welding speed of 100 amp and the hardness obtained is more as compared to all other cases of Fig. 10. It clearly shows that with less current and increasing weld speed the hardness can be increased and with increased current it can enlarge the weld bead and in turn distortion. Figure 10 (Graph C) shows changes of hardness with welding speed at 300 amp and from this graph it is seen that the hardness is less as compared to 200 amp and 100 amp. This results in the less hardness of the
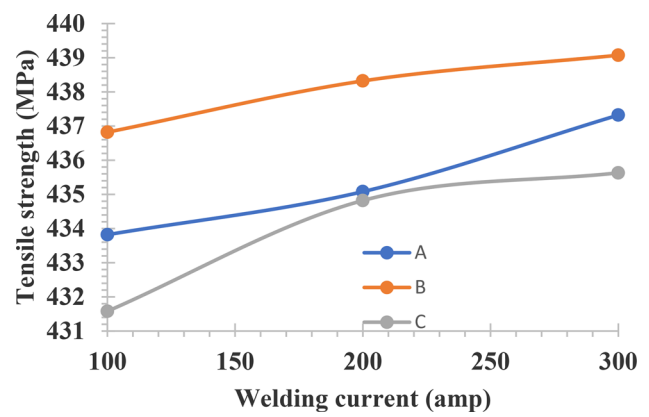
material and occurring due to increase in current and speed of weld.

Table 5 shows the Brinell hardness test results for various samples considered for the study. From this Table 4, it is seen that maximum hardness is achieved with 200 amp welding current and welding speed of 4 mm/min and lowest hardness is seen at 5 mm/min welding speed with 300-amp welding current.

5.4 Tensile strength

5.4.1 Welding current effect on tensile strength

Tensile strength on the samples have been performed using FIE make Universal testing machine, UTES-10. Figure 11 depicts the effect of ultimate tensile strength for specimens for welding current considering various gas flow rates and speeds. It is observed that highest tensile strength is achieved at 300 amp and from the graph it is observed that strength

Table 5 Brinell hardness test results

Sample No	Welding on plates	Gas flow rate (L/min)	Current (amp)	Speed (mm/min)	Hardness (HRB)
1	1–2	20	100	4	77
2	3–4	10	100	3	76
3	5–6	15	100	5	75
4	7–8	20	200	4	80
5	9–10	10	200	3	79
6	11–12	15	200	5	77
7	13–14	20	300	4	75
8	15–16	10	300	3	74
9	17–18	15	300	5	73

(ultimate) of the material is continuously increasing with rise in welding current.

This occurs due to more heat as the current is increasing, it in turn affects the microstructure of test specimen and homogeneous cooling of the material and proper fusing of filler material into the base metal. Increasing the current increases, the depth of penetration and higher penetration depth increases more melting of base metal and in turn gives higher tensile stress as described by Hussian et al. [28]. At high gas flow rate, the amount of gas surrounding the weld pool is more and reduces the oxidation of oxygen and other gases and it protects the welding surface and is one of the most important aspects of welding. So, it can be stated that low gas flow rate helps to increase the tensile strength of the material and higher gas flow rate tends to decrease the tensile strength of the material. Figure 11 (Graph A) shows the changes of welding current and ultimate tensile strength, and it is observed that the ultimate tensile strength is 434 MPa for welding current of 100 amp. This occurs due to reduction in welding speed of 3 mm/min and reduction of flow rate to 10 L/min and in turn less ultimate tensile strength but increases with welding current. Figure 11 (Graph B) shows the influence of welding current and tensile strength for 20 L/min flow rate and 4 mm/min welding speed and has ultimate strength more as compared to other cases. In this case as the flow rate is high and welding speed is 4 mm/min, it causes decrease in peak temperature and maximum velocity in the welding zone which reduces weld pool dimensions and decrease in the size (width) of the heat affected zone. Similarly, we can observe the decrease in ultimate tensile strength from Fig. 11 (Graph C) due to decrease in flow rate to 15 L/min and increase in welding speed to 5 mm/min.

5.4.2 Welding speed effect on tensile strength

The welding speed refers to the travel speed of the arc during welding and is the relative speed with respect to the workpiece. Figure 12 shows the graph of ultimate tensile strength of specimens for changes in welding speed.

From the above Fig. 12 it is observed that tensile strength reduces with increase in welding speed for all the cases considered. For a particular given current if the travel speed is slower will helps to produce larger bead and more heat supply to the base metal due to prolonged heating time. This longer heating time helps to increase the penetration of the weld and accumulates more metal per unit length and results in wider weld area. This also results in more heat transfer near the weld pool surface and heat affected zone (HAZ). Similarly, if the speed of travel is lower, the weld built up will be more which fails to fuse properly with the weld metal, less penetration with the weld metal and possibility of slag inclusion and uneven bead width. From Fig. 12 (Graph A) the ultimate tensile strength of the material is less as compared
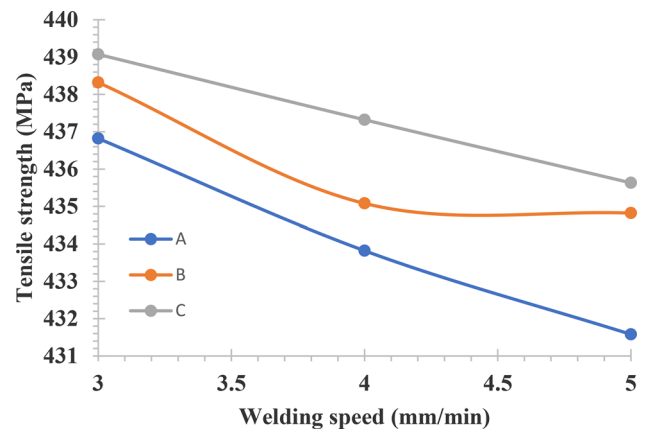

Fig. 12 Variation of tensile strength of specimens with welding speed, **A**—welding current 300 amp, **B**—welding current 200 amp, **C**—welding current 100 amp
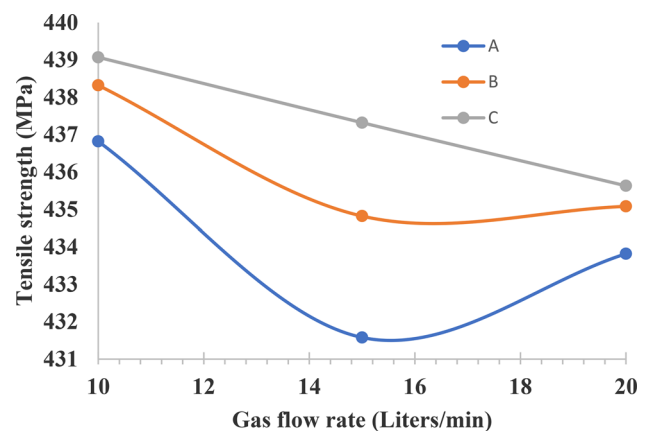

Fig. 13 Changes of tensile strength with gas flow rate, **A**—welding current 300 amp, **B**—welding current 200 amp, **C**—welding current 100 amp

to other cases (Fig. 12 Graph B and Graph C). This is due to the increase in the current to 300 amp which widens the weld bead and increased distortion. Excessive current causes overheat in the welding electrode causing instability which in turn leads to undercutting.

The tensile strength is less at welding speed (5 mm/min at 100 amp current and 1.5 L/min gas flow rate) and results in welding defects such as trapping of gases with the metal weld pool and occurs due to improper penetration.

5.4.3 Gas flow rate effect on tensile strength

Figure 13 shows the difference of ultimate tensile strength of specimens welded for changes in gas flow rate for changes in welding current and welding speeds.

In all the cases it is observed that the maximum tensile strength is encountered at minimum gas flow rate. So, increase in gas flow rate will help the weld material to be protected against atmospheric contamination giving high quality weld as specified by Bitharas et al. [29]. But from the Fig. 13

(Graph C) it is observed that maximum tensile strength is achieved at less welding current and minimum gas flow rate. As the welding current increases the tensile strength increases up to an optimal value of welding current and it decreases as the welding current increases as mentioned by Edwin et al. [30]. Hence, in this case of Fig. 13 (Graph C) the ultimate strength is highest as compared to other graphs of Fig. 13 and helps to increase the weld joint performance. The tensile strength decreases as welding current increases due to amount of base metal melted, depth of diffusion, rate at which welding electrode melted etc.

Figure 13 (Graph A) shows increase in tensile strength after gas flow rate of 15 L/min for a welding current of 300 amp. This happens due to increase in the gas flow rate which protects the welding zone from atmospheric contamination and slight increase in tensile strength is achieved as the welding current is high in this case. Table 6 shows the tensile strength for various samples considered for the study. The maximum hardness is achieved at 300 amp with 10 L/min gas flow rate.

6 Taguchi method

Design of experiments using Taguchi design is one of the techniques commonly and widely used for Design of experiments (DOE). The Taguchi method helps to optimize the variation for various parameters considering robust design of experiments. The main objective is to manufacture high quality products with less cost of production. This method also helps us to improve the performance and reliability of these welding process used in case of railway structures as well as it utilizes both average and variation of data as compared to average values used in traditional method which ensures better results with minimum variance. He developed the design of experiments to investigate the effects of different parameters and its effects on mean and variance and to check the level of performance during the functioning of these processes. Taguchi proposed the experimental design using orthogonal arrays to study the parameters affecting the processes at various levels when it is varied. Taguchi's orthogonal array helps to design experiments considering a subset of combinations using multiple variables at multiple levels. An orthogonal array is the balanced design considered for various factor levels to weigh each factor equally so that each factor can be estimated independently with respect to the other factor considered for the experiments. This method also evaluates each factor independently in such a way that the effect of one variable does not influence the estimation of another variable. Minitab Software version 21.1.1 has been used to process S/N Ratio and results are as explained below:

Table 7 Control parameters and S/N ratios for ultimate tensile strength (Larger is better)

Level	Welding Current (amp)	Welding Speed (mm/min)	Gas Flow rate (Litres/min)
1	52.75	52.83	52.83
2	52.79	52.78	52.75
3	52.82	52.75	52.78
Delta	0.07	0.08	0.08
Rank	3	1.5	1.5

6.1 Evaluation of S/N ratios

The S/N ratios were calculated using Taguchi's methodology. The S/N ratio is the signal to noise ratio in which 'signal' is the desirable value (mean) and the 'noise' is the undesirable value (standard deviation). It clearly demonstrates the amount of variation present in the performance characteristic. There are various types of S/N ratios depending upon the objective of the performance characteristic. Here the desirable objective is greater values of tensile strength. Hence the greater-the-better (HB) type S/N ratio was used to transform the raw data. (Mohan et al. [31]).

$$(S/N)_{HB} = -10 \, log_{10} \frac{1}{n} \sum_{i=1}^{n} \frac{1}{y_i^2} \qquad (7)$$

where y_j is the value of the characteristic in a set of observation j and R is the number of observations or the number of repetitions in a trial (Srinivasa et al. [32]).

6.2 Estimation of optimal parameter selection from S/N ratios for ultimate tensile strength

The Experimental value for the ultimate tensile strength and the response values of S/N ratios are presented in Table 7. The corresponding graphical value of S/N ratios for corresponding welding parameters are presented in Fig. 14. From this Fig. 14 it is possible to observe the optimised values for welding parameters considered for the study to know the maximum ultimate tensile strength. The main effects plots of welding current, welding speed and gas flow rate is shown in Fig. 14. From this it is seen that ultimate tensile strength increases when welding current increases from 100 to 300 amp. Therefore, the optimum value for welding current is 300 amp. Similarly, the ultimate tensile strength decreases for welding speed from 3 to 5 mm/min and the optimum value for welding speed is 3 mm/s. Also, the ultimate tensile strength decreases for gas flow rate of 10–15 L/min and increases to 20 L/min and the optimum value for gas flow rate is 10 L/min. From the main effect plots from means of

Table 6 Tensile strength test results

Sample No	Welding on plates	Gas flow rate (L/min)	Current (amp)	Speed (mm/min)	Ultimate tensile strength (MPa)
1	1–2	20	100	4	433.82
2	3–4	10	100	3	436.82
3	5–6	15	100	5	431.58
4	7–8	20	200	4	435.08
5	9–10	10	200	3	438.32
6	11–12	15	200	5	434.82
7	13–14	20	300	4	437.32
8	15–16	10	300	3	439.07
9	17–18	15	300	5	435.63

Fig. 14 the value of delta is higher for welding speed, gas flow rate and then followed by welding current and it shows the significance of welding speed, gas flow rate as compared to welding current.

6.3 Estimation of optimal parameter selection from S/N ratios for hardness

The Experimental value for the hardness and the response values of S/N ratios are tabulated in Table 8. The corresponding graphical value of S/N ratios for corresponding welding parameters are presented in Fig. 15. From this Fig. 15 it is possible to observe the optimized values for welding parameters considered for the study to know the hardness. The main effects plots of welding current, welding speed and gas flow rate is shown in Fig. 15. From this it is observed that hardness increases when the welding current increases from 100 to 200 amp and then the hardness decreases for welding current of 300 amp. Therefore, the optimum value of hardness is 200 amp. Similarly, the hardness increases for welding speed

Table 8 Control parameters and S/N ratios for hardness (Smaller is better)

Level	Welding current (amp)	Welding speed (mm/min)	Gas flow rate (L/min)
1	− 37.62	− 37.65	− 37.65
2	− 37.91	− 37.76	− 37.50
3	− 37.38	− 37.50	− 37.76
Delta	0.53	0.27	0.27
Rank	1	2.5	2.5

of 3 mm/min to 4 mm/min and then it decreases for 5 mm/s and the optimum value for welding speed is 4 mm/min. Also, the hardness decreases for gas flow rate of 10–15 L/min and then increases for 20 L/min and the optimum value for gas flow rate is 20 L/min. From the main effect plots from means of Fig. 15 the value of delta is higher for welding current and then followed by welding speed and gas flow rate and the significant parameter for hardness is welding current.
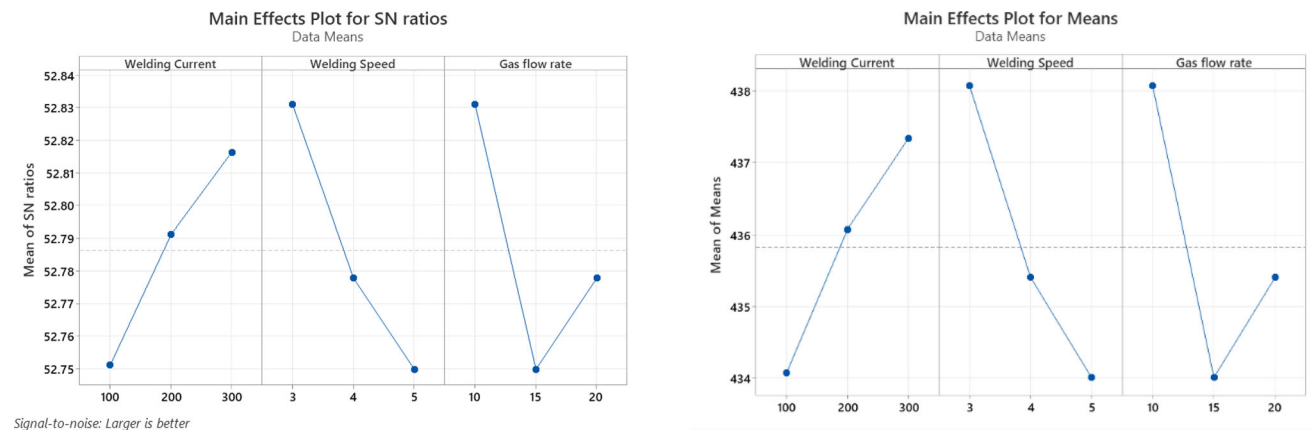
Fig. 14 Plot for S/N ratios and means of ultimate tensile strength for varying welding current, welding speed and gas flow rate
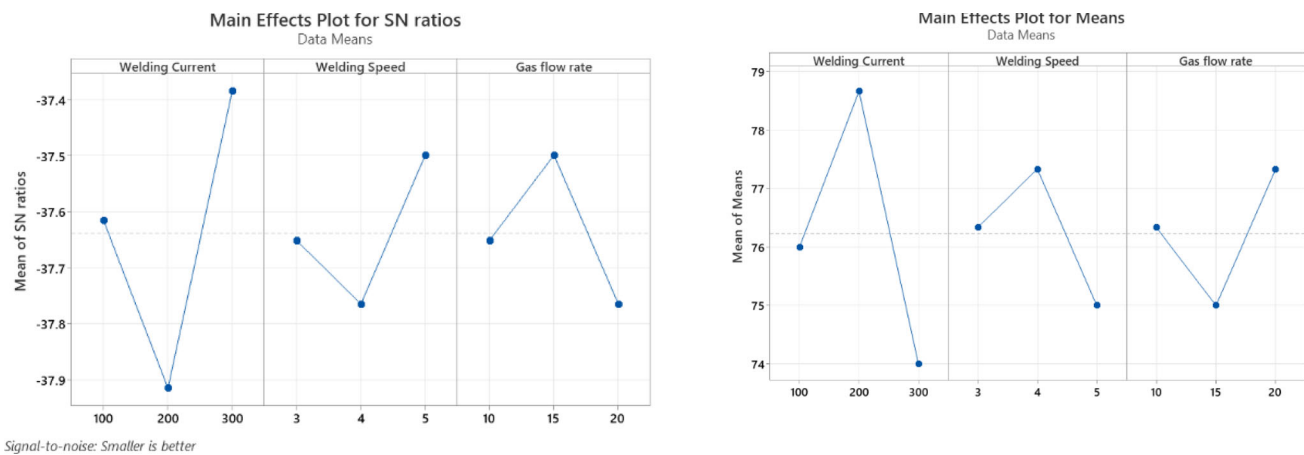
Fig. 15 Plot for SN ratios and means of hardness for welding current, welding speed and gas flow rate for hardness

7 Conclusion and scope for the future work

In this research article an attempt was made to study the hardness and welding strength or tensile strength of the welded joints of steel materials considering various parameters of welding such as welding current, gas flow rate and welding speed. Some of the conclusions drawn by the experimentation and the design of experiments are presented below.

- At lower gas flow rate welded specimens shows higher tensile strength and less ductility and occurs due to lowering of the heat at welding zone. At higher welding speed, there is more chances of welding defects, and the penetration is improper due to the low heat input in the weld pool.
- Based on experimental results the highest hardness was achieved for specimen 7–8 for Gas flow rate of 20 L/min, 200-amp welding current and speed of 4 mm/min. This occurs due to the increase in gas flow rate which helps to protect the weld and weld material against atmospheric contamination.
- Based on experimental results the highest ultimate tensile strength was achieved for specimen 15–16 for gas flow rate of 10 L/min, 300 amp current and welding speed of 3 mm/min. As the gas flow rate increases it protects the welding zone from atmospheric contamination and in turn increase in tensile strength is observed.
- Based on Taguchi optimization, the optimum value for hardness is 200 amp for welding current, 4 mm/min for welding speed and 20 L/min for gas flow rate and these results are matching with that of experimental results.
- Based on Taguchi optimization, the optimum value for ultimate tensile strength is 300 amp for welding current, 3 mm/min for welding speed and 10 L/min for gas flow rate and these results are matching with that of experimental results.
- The optimal parameters for ultimate strength are the gas flow rate and welding speed as compared to welding current and the optimal parameters for hardness are the welding current followed by welding speed and gas flow rate.

Future Scope.

- In this research article, the study is done for a particular thickness in case of car body structures of railway. This work can be extended for various materials with varying thickness.
- The microstructural analysis of the weld structure can also be studied by examining different samples using scanning electron microscope or optical microscope and the effect of these microstructures on mechanical properties can be studied.
- This study can be applied in automobiles structures where the thickness of the weld specimen is negligible.

Declarations

References

1. Charles, C.I., Reyazul, H.K., Joseph, A., Sunday, A.L., Nicholas, O.N.: Effect of tungsten inert gas welding parameters on the performance of AISI 304 alloy steel using multi-response optimization technique. Weld. Int. **35**(1–3), 45–55 (2021). https://doi.org/10.1080/09507116.2021.1958660
2. Tsung, Y.K., Yen, T.L.: Effect of shielding gas flow rate and power Waveform on Nd:YAG laser welding of A5754-O aluminium alloy. Mater. Trans. **47**(5), 1365–1373 (2006)

3. Masahiro, O., Takashi, M., Kanto, M., Tadahisa, T., Kohei, F.: A new approach to controlling metal transfer by dynamic modification in gas composition of arc atmosphere: studies on pulsed gas MAG welding. Weld. Int. **34**(10–12), 430–454 (2020). https://doi.org/10.1080/09507116.2021.1936927

4. Harsh, S., Balram, R., Rudra, P.S.: A review paper on effect of input welding process parameters on structure and properties of weld in submerges arc welding process. Mater. Today: Proc. **26**(2020), 1931–1935 (2020). https://doi.org/10.1016/j.matpr.2020.02.422

5. Yemelyushin, A.N., Sychkov, A.B., Manin, V.P., Sheksheyev, M.A.: Investigation of the structure and mechanical properties of welded joints in steels of the K56 strength grade in different welding conditions. Weld. Int. **28**(1), 70–74 (2013). https://doi.org/10.1080/09507116.2013.796658

6. Mei, Y., Jingxiang, L., Jing, C., Yang, L., Honglang, Y.: Effect of welding speed on microstructure and corrosion resistance of Al–Li alloy weld joint. Mater. Corros. **71**(2), 300–308 (2019). https://doi.org/10.1002/maco.201911068

7. Wichan, C., Loeshpahn, S.: Heat input and shielding gas effects on the microstructure, mechanical properties and pitting corrosion of alternative low cost stainless steel grade 202. Res. Mater. **7**(2020), 1–9 (2020). https://doi.org/10.1016/j.rinma.2020.100111

8. Xin, Y.Z., Xiao, Q.Z., Ling, Q.G., Peng, H.H., Yong, F.R.: Influence of shielding gas on microstructure and properties of GMAW DSS2205 welded joints. Materials **14**(10), 2671 (2021). https://doi.org/10.3390/ma14102671

9. Ajit, H., Ashwani, D., Satpal, S.: Optimization of MIG welding process parameters to predict maximum yield strength in AISI 1040. Int. J. Mech. Eng. Robot. Res. **1**(3), 203–213 (2012)

10. Chinakhov, D.A., Grigorieva, E.G., Mayorova, E.I., Kartsev, D.S.: The influence of shielding gas flow rate on the transfer frequency of electrode metal drops. In: International Scientific Practical Conference "Innovative Technologies in Engineering", vol. 142, pp. 1–6 (2016). https://doi.org/10.1088/1757-899X/142/1/012005

11. Xiaoyi, Y., Hui, C., Zongtao, Z., Chuang, C., Chenhzhu, Z.: Effect of shielding gas flow on welding process of laser-ac hybrid welding and MIG welding. J. Manuf. Process. **38**(2019), 530–542 (2019). https://doi.org/10.1016/j.jmapro.2019.01.045

12. Liu, S., Cui, B., Bai, D., Yan, S., Zhanh, H.: Effect of N_2 shielding gas flow rate on microstructure and weld surface corrosion resistance of high nitrogen steel by laser-arc hybrid welding. Mater. Res. Expr. **6**(8), 1–8 (2019). https://doi.org/10.1088/2053-1591/ab29b7

13. Maros, V., Miroslav, S., Maria, D., Peter, J., Martin, S., Monika, V., Maros, M.: The effect of process parameters on the microstructure and mechanical properties of AW5083 aluminium laser weld joints. Metals **10**(11), 1–22 (2020). https://doi.org/10.3390/met10111443

14. Rahman, M.N.A., Zulkipli, N.H., Kasim, M.S., Jamli, M.R., Budi, E.: Impact of argon gas shielding flow rate on the hardness of weld joint. J. Adv. Manuf. Technol. **16**(1), 1–10 (2022)

15. Ashish, G., Hardik, K., Lade, J., Kuldeep, K.S., Ummal, N.S., Kahtan, A.M.: Experimental investigation to analyse the mechanical and microstructure properties of 310 SS performed by TIG welding. Adv. Mat. Sci. Eng. **2022**, 1–11 (2022). https://doi.org/10.1155/2022/1231843

16. Leander, S., Klaus, S., Jean, P.B., Christina, J.: Effect of local gas flow in full penetration laser beam welding with high welding speeds. Appl. Sci. **10**(5), 1–19 (2020). https://doi.org/10.3390/app10051867

17. Anteneh, T.A., Gulam, M.S.A., Sagr, A., Abhilash, E., Moera, G.J., Vivek, P., Nazia, H.: Experimental investigation and parametric optimization of the tungsten inert gas welding process parameters of dissimilar metals. Materials **15**(13), 1–30 (2022). https://doi.org/10.3390/ma15134426

18. Rizvi, S.A., Tewari, S.P.: Effect of shielding gas flow rate on mechanical properties and microstructure of structural steel (IS2062) welds. Mech. Mech. Eng. **21**(4), 1–14 (2017)

19. Viktor, A.R., Nikita, V.M., Vladislav, V.K., Vadim, S.T., Viktor, A.K., Anna, V.G., Vadim, Y.S., Anatoly, V.L., Antonina, I.K.: Study of melting methods by electric resistance welding of rails. Metals **12**(12), 2135 (2022). https://doi.org/10.3390/met12122135

20. Piotr, W., Mariusz, N., Stanislaw, K.: Experimental studies of welded joints in structures subjected to high impact vibrations using destructive and destructive methods. Materials (Basel) **16**(5), 1886 (2023). https://doi.org/10.3390/ma16051886

21. Takeshi, K., Toshiaki, M., Kentarou, M., Hideshi, O., Yoshihiko, I., Masakuni, E.: Application of friction stir welding to construction of railway vehicles. JSME Int. J. **47**(3), 503–511 (2004)

22. Bekir, C., Behcet, G.: The effect of welding speed on mechanical and microstructural properties of 5754 AL (AlMg$_3$) alloy joined by laser welding. Mater. Res. Expr. **5**(8), 1–5 (2018)

23. Muyu, L., Dan, Y., Yingping, G., Yongchuan, D., Liu, Y.: Effect of welding speed and post quenching on the microstructure and mechanical properties of laser-welded B1500HS joints. Materials **2020**(13), 1–16 (2020). https://doi.org/10.3390/ma13204645

24. Panji, M., Baskoro, A.S., Widyianto, A.: Effect of welding current and welding speed on weld geometry and distortion in TIG welding of A36 mild steel pipe with V-groove joint. IOP Conf. Ser.: Mater. Sci. Eng. **694**(2019), 1–8 (2019). https://doi.org/10.1088/1757-899X/694/1/012026

25. Zhao, Y.Y., Zhang, Y.S., Hu, W.: Effect of welding speed on microstructure, hardness and tensile properties in laser welding of advanced high strength steel. Sci. Technol. Weld. Join. **18**(7), 581–590 (2013). https://doi.org/10.1179/1362171813Y.0000000140

26. Ahmad, J.K., Dhia, C.A., Abass, H.L.: Effect of metal inert gas welding parameters on the hardness and bending strength of carbon steel plates. AIP Conf. Proc. **2372**(1), 1–8 (2021). https://doi.org/10.1063/5.0066092

27. Morakabiyan, M., Farzadi, A., Alavi, Z.S.R.: Effect of welding speed on gas metal arc weld pool in commercially pure aluminium: theoretically and experimentally. Phys. Metall. Heat Treat. **59**(2018), 82–92 (2018). https://doi.org/10.3103/S1067821218010121

28. Hussian, Z., Muhammad, A.J., Anasyida, A.S., Suhaina, I.: Welding investigation and prediction of tensile strength of 304 stainless steel sheet metal joint by surface response methodology. Proc. Chem. **19**(2016), 217–221 (2016). https://doi.org/10.1016/j.proche.2016.03.09

29. Bitharas, I., McPherson, N.A., McGhie, W., Roy, D., Moore, A.J.: Visualization and optimisation of shielding gas coverage during gas metal arc welding. J. Mater. Process. Technol. **255**(2018), 451–462 (2018). https://doi.org/10.1016/j.jmatprotec.2017.11.048

30. Edwin, R.D.J., Jenkins, H.D.S.: A review on optimization of welding process. Proc. Eng. **38**(2012), 544–554 (2012). https://doi.org/10.1016/j.proeng.2012.06.068

31. Mohan, K.S., Rajesh, K.A., Pramod, R., Siva, S.N., Dhinakaran, V.: Testing, characterization and numerical prediction (uni-axial tension and bend test) of double side TIG welded SS321 plates for pressure vessel applications. Int. J. Press. Vessel. Pip. **197**(2022), 104648 (2022). https://doi.org/10.1016/j.ijpvp.2022.104648

32. Srinivasa, R.V., Brahma, R.K., Venkata, S.K.: Optimization of welding parameters of Ti 6al 4v cruciform shape weld joint to improve weld strength based on Taguchi method. Mater. Today: Proc. **5**(2018), 4948–4957 (2018). https://doi.org/10.1016/j.matpr.2017.12.072